Limitations and opportunities of off-shell coupling measurements

Christoph Englert[1,*] and Michael Spannowsky[2,†]

[1]SUPA, School of Physics and Astronomy, University of Glasgow, Glasgow G12 8QQ, United Kingdom
[2]Institute for Particle Physics Phenomenology, Department of Physics, Durham University, Durham DH1 3LE, United Kingdom

(Received 12 May 2014; published 3 September 2014)

Indirect constraints on the total Higgs width Γ_h from correlating Higgs signal strengths with cross-section measurements in the off-shell region for $p(g)p(g) \to 4\ell$ production have received considerable attention recently, and the CMS Collaboration have published a first measurement. We revisit this analysis from a new physics and unitarity constraints perspective and conclude that limits on Γ_h obtained in this fashion are not reliable unless we make model-specific assumptions, which cannot be justified at the current stage of the LHC program. Relaxing the Γ_h interpretation, we discuss the merits of high invariant mass cross-section measurements in the context of Higgs $\mathcal{CP}$ analyses, higher-dimensional operator testing, and resolved new physics in the light of electroweak precision constraints beyond effective theory limitations. Furthermore, we show that a rather model-independent LHC constraint can be obtained from adapting the $gg \to 4\ell$ analysis to the weak boson fusion channels at lower statistical yield.

DOI: 10.1103/PhysRevD.90.053003 PACS numbers: 14.80.Bn, 12.60.-i

I. INTRODUCTION

After the 2012 discovery [1,2], the ATLAS and CMS collaborations have scrutinized the SM interpretation of the Higgs candidate within the boundaries of the currently available data. A strong resemblance of the particle's properties with the SM Higgs expectation has emerged: it is likely to be a $\mathcal{CP}$-even scalar boson, and its "signal strengths"

$$\mu_{i,j} = \frac{\sigma_{h,i} \times \mathrm{BR}_j}{[\sigma_{h,i} \times \mathrm{BR}_j]^{\mathrm{SM}}} \sim \frac{\Gamma_i \Gamma_j}{\Gamma_i^{\mathrm{SM}} \Gamma_j^{\mathrm{SM}}} \frac{\Gamma_h^{\mathrm{SM}}}{\Gamma_h} \tag{1}$$

are in good agreement with the SM Higgs boson. i, j in Eq. (1) refer to the different Higgs production and decay modes that have been observed so far. For fully inclusive measurements, they can be related to the partial decay widths $\{\Gamma_i\}$. "Higgsistence" has mainly been established from gluon fusion, the largest Higgs production mechanism in the SM.

The apparent agreement of the measured quantities of Eq. (1) with the SM predictions highlights the question of whether the discovered particle is indeed the Higgs boson as predicted by the SM.

On the one hand, unitarity largely constrains the bare couplings of massive fermions and gauge bosons to $\mathcal{CP}$-even Higgs boson(s) in the SM. If the absolute values of the Higgs candidate's couplings are close to the SM predictions, there will be little room left for resonant physics beyond the SM (BSM) in e.g. the weak boson fusion (WBF) channels, which is a direct probe of longitudinal gauge boson scattering.

On the other hand, absolute values of couplings are difficult to infer at hadron colliders, since signal strength measurements involve nonlinear relations among the couplings and $\sigma \times \mathrm{BR}$ phenomenology leaves the total Higgs width as a flat direction in coupling fits. This is usually overcome by making assumptions about the total Higgs width in these fits [3], or, alternatively, about the maximum coupling value of the Higgs candidate to gauge bosons [4], which is determined by the Higgs' gauge representation. The biases that are introduced in either of these approaches are far from being well motivated at the current stage.

Assuming $\Gamma_h \simeq \Gamma_h^{\mathrm{SM}} \simeq 4$ MeV skews coupling fits towards a parameter region that is oblivious of the Higgs bosons' potential interplay with dark matter phenomenology [5] and other phenomena that can be introduced via well-motivated portal-type interactions [6,7].

Assumptions about the Higgs $SU(2)_L$ representation are usually limited to the **2**'s due to the (accidental) custodial isopin symmetry that preserves $T \simeq 1$ in (multi-)Higgs doublet models. However, it is known that both current signal strength measurements and electroweak precision constraints can be accounted for in models with nondoublet Higgs fields [8], and the complementing searches for Higgs exotics [9] necessary to rule out such an option are not available yet.

Obviously, a model-independent constraint on Γ_h [or BR(invisible) if a particular model leaves production modes unaltered] has a huge impact on BSM physics.[1] Hence, it is not surprising that the recent proposal by Caola

*christoph.englert@glasgow.ac.uk
†michael.spannowsky@durham.ac.uk

[1]See e.g. Ref. [5] for a discussion of the invisible branching ratio measurements, e.g. Ref. [10], in relation with dark matter phenomenology.

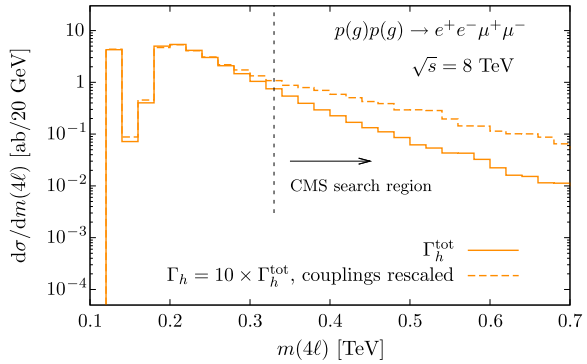

FIG. 1 (color online). Constraining the total Higgs width by fixing the signal strength (on-shell region) and measuring the cross section at large invariant ZZ masses, keeping couplings in the on-shell and Higgs off-shell region fixed. Distributions are leading order, while keeping all quarks dynamical and the bottom and top quarks massive. We have chosen a minimal cut set $p_T(\ell) \geq 10$ GeV, $|y(\ell)| \leq 2.5$, $\Delta R(\ell\ell') \geq 0.4$.

and Melnikov [11] that interprets off-shell cross section measurements of $pp \to 4\ell$ [12] as a probe of Γ_h has received considerable attention [13–15].[2] Just recently, CMS have presented first results [18] using this strategy, claiming $\Gamma_h < 4.2 \times \Gamma_h^{\rm SM}$ at a 95% confidence level by injecting a global Higgs signal strength $\mu \simeq 1$. The strategy is sketched in Fig. 1, and we give a quick outline to make this work self-contained (for additional details see Refs. [11,14,18]):

As long as the narrow width approximation is applicable, the cross section for the process $p(g)p(g) \to h \to ZZ^* \to 4\ell$ in the Higgs on-shell region scales as[3]

$$\sigma_{h,g} \times \mathrm{BR}(H \to ZZ \to 4\ell) \sim \frac{g_{ggh}^2 g_{hZZ}^2}{\Gamma_h}, \tag{2}$$

where we denote the relevant couplings by g_X. The dominant Feynman diagram in this phase space region is the triangle of Fig. 2; the continuum contribution from $gg \to ZZ^*$ is highly suppressed, and interference is negligible [12].

Since the Higgs width is anticipated to be a small parameter compared to the Higgs mass $\Gamma_h/m_h \sim 10^{-4}$, we can expand the Higgs Breit-Wigner propagator $\mathcal{D}(s) = i/(s - m_h^2 + i\Gamma_h m_h)$ away from the peak region $s \gg m_h^2$:

$$|\mathcal{D}|^2 = \frac{1}{s^2}\left(1 + \frac{m_h^4}{s^4}\frac{\Gamma_h^2}{m_h^2}\right) + \mathcal{O}\left(\frac{\Gamma^4}{s^4}\right), \tag{3}$$

which shows that the Higgs width parameter rapidly decouples from the scattering process for Higgs off-shell production. Therefore, the contribution from the triangle diagrams in Fig. 2 (neglecting interference for the moment) scales as

[2]Similar strategies [16] have been proposed for $h \to \gamma\gamma$ [17].

[3]We mainly focus on the final state $e^+e^-\mu^+\mu^-$ in the following. Generalizing our results to full leptonic ZZ decays is straightforward due to negligible identical fermion interference.

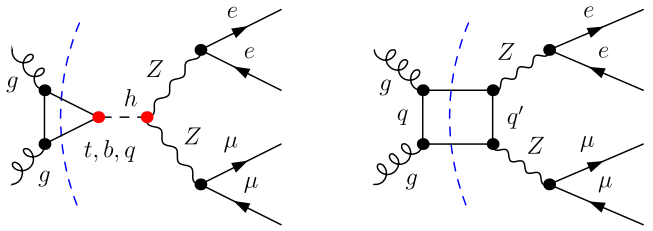

FIG. 2 (color online). Representative Feynman diagram topologies contributing to $gg \to ZZ$ with leptonic Z-boson decays in the SM and theories with extended fermionic sectors.

$$\mathrm{d}\bar{\sigma}_h \sim \frac{g_{ggh}^2(\sqrt{s})\, g_{hZZ}^2(\sqrt{s})}{s}\, \mathrm{dLIPS} \times \mathrm{pdfs}. \tag{4}$$

Now, if there is a direct correspondence between $g_i(m_h)$ and $g_i(\sqrt{s})$, measuring the signal strength μ in the off-shell and on-shell regions simultaneously allows us to set a limit on the width of the Higgs boson Γ_h. More explicitly, for $\Gamma_h > \Gamma_h^{\rm SM}$, we need to have $g_{ggh}^2 g_{hZZ}^2 > (g_{ggh}^2 g_{hZZ}^2)^{\rm SM}$ to keep $\mu = \mu^{\rm SM}$ fixed, which in turn implies $\bar{\sigma}_h > \bar{\sigma}_h^{\rm SM}$. Figure 1 validates this line of thought and qualitatively reflects the CMS analysis.

But how general is this approach, or put differently, how solid is a limit on Γ_h obtained this way once we include unknown new physics effects? And letting aside the interpretation in terms of a constraint on the Higgs width, what are the more general ramifications of a measurement of the gluon-fusion ZZ and WW cross section away from the Higgs mass peak?

It is the purpose of this paper to address these questions from a new physics perspective with a particular emphasis on probability conservation. First, we interpret the outlined Higgs width measurement from a unitarity perspective, which paves the way to the formulation of a simple and transparent BSM counterexample. We analyze the interplay of new resolved physics contributions to $gg \to VV^*$ to both Higgs and continuum ZZ, WW production in light of electroweak precision constraints and finally point out that, enforcing $\mu \simeq \mu^{\rm SM}$, the off-shell measurement provides additional statistical pull to constrain the Higgs' $\mathcal{CP}$ nature in the presence of higher-dimensional operators (unresolved new physics). We also discuss off-shell measurements in WBF in Sec. V.

As we will see, in order to gain qualitative control of new physics effects in the Higgs off-shell region, we cannot rely on effective theory calculations for the SM spectrum. We consequently keep all quarks dynamical and include finite mass effects of the bottom and top quarks. Our work therefore extends beyond the assumptions of Ref. [19], which has discussed the impact of new operators to high invariant mass measurements in detail recently. We only focus on modified ggh and hZZ/hWW interactions and neglect QED contributions throughout; they are negligible for high invariant masses when both Z's are fully

reconstructed, but can be sensitive to the presence of new physics when studied on the Higgs peak via $h \to Z\gamma^*, \gamma^*\gamma^*$ [20]. We will mainly focus our discussion on $\sqrt{s} = 8$ TeV; our results straightforwardly generalize to run II.

Computations have been performed and cross-checked with a combination of FeynArts/FormCalc/LoopTools [21], Helas [22], MadGraph/MadEvent [23], and Vbfnlo [24]. We have checked our results against Ref. [13] and find very good agreement.

II. HIGGS WIDTH MEASUREMENTS FROM $gg \to VV$: A UNITARITY PERSPECTIVE

In Fig. 3 we show the individual contributions of $pp \to ZZ^* \to e^+e^-\mu^+\mu^-$ that result from the Feynman diagrams of Fig. 2. We also include a comparison of the full Higgs contribution with the low-energy effective theory [25] as implemented in MadGraph/MadEvent [23], which shows large deviations when the absorptive parts of the top quark loop are resolved (the corresponding Cutkosky cut [26] is included in Fig. 2). Obviously, a reliable analysis of the high invariant mass region in correlation with the on-shell part cannot be obtained by applying effective theory simplifications. The CMS analysis [18] focuses on $m(4\ell) \geq 330$ GeV.

It is known that the interference between the triangle and box diagrams is destructive [12] above the $2m_t$ threshold. This large interference effect becomes transparent when calculating the cross section for the process $q\bar{q} \to ZZ$ with massive quarks in the initial state. It involves a highly nontrivial cancellation between the gauge and Yukawa sector interactions in $q\bar{q} \to Z_L Z_L$ [27], and is part of the

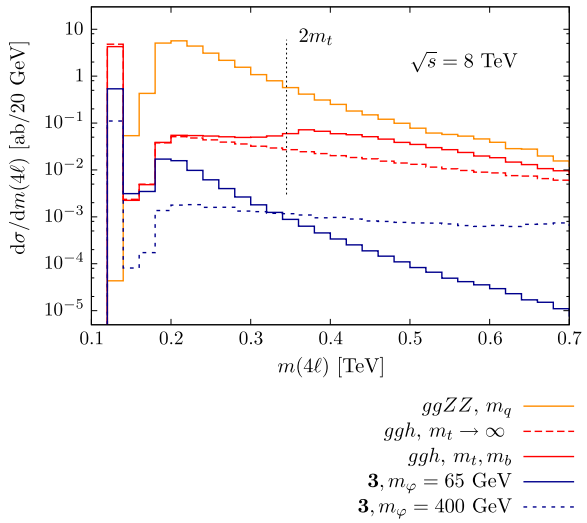

FIG. 3 (color online). Individual leading-order contributions from Fig. 2 to the full hadronic cross section. For comparison we also include the effective theory distribution resulting from a ggh effective vertex in the $m_t \to \infty$ limit. Cuts are identical to Fig. 1. The colored scalars are for representative values of λ and Γ_h to illustrate their behavior. For additional details, see text.

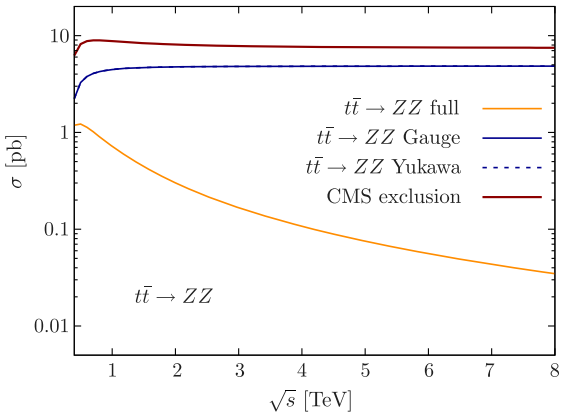

FIG. 4 (color online). Unpolarized $t\bar{t} \to ZZ$ cross section as a function of energy. We demonstrate unitarity cancellations between the gauge and Yukawa-type interactions (blue solid and dashed; the dashed line lies on top of the solid line), yielding a well-defined SM cross section (orange). We also show the parameter choice that corresponds to the CMS-like exclusion of $\Gamma_h \simeq 5 \times \Gamma_h^{\mathrm{SM}}$ based on the strategy outlined in Ref. [2] and the Introduction.

absorptive $gg \to ZZ$ amplitude according to the branch cuts shown in Fig. 2. Even though both contributions are gauge invariant under QCD transformations, they are related by weak gauge invariance, and only their coherent sum with SM-like couplings is well defined.

In Fig. 4, this is demonstrated for the unpolarized $t\bar{t} \to ZZ$ cross section: The s-channel Yukawa couplings of $\bar{t}_L t_R h + \mathrm{H.c.}$ conspire via a coupling relation with the weak gauge interactions $g_L \bar{t}_L Z t_L + g_R \bar{t}_R Z t_R$ when $-t, -u \sim s$. A simple rescaling of one part of the amplitude is tantamount to unitarity violation in the fermion-gauge interactions. This leaves a crucial question of the limit obtained in Ref. [18]: Is the theory underlying the width constraint well defined?

The alert reader might object at this stage that such a question, in fact, is also well motivated for Higgs coupling measurements as performed by ATLAS and CMS [28] when Higgs couplings are varied independently throughout the SM Lagrangian. This is certainly true if one would like to understand deviations from an electroweak precision point of view. However, the situation for Higgs $\sigma \times \mathrm{BR}$ phenomenology is fundamentally different. The relevant scale at which couplings are evaluated is the Higgs mass, and $\sigma \times \mathrm{BR}$ phenomenology is manifestly free of UV problems to leading order in the electroweak perturbative series expansion.[4] This needs to be contrasted with an off-shell measurement that integrates over an invariant-mass region $2m_t \lesssim m(4\ell) \leq 1.6$ TeV [18].

To address this question quantitatively, we show the zeroth partial wave projection as a function of the partonic

[4]This will dramatically change when the measurements of differential weak boson fusion distributions will be scrutinized at high precision [29].

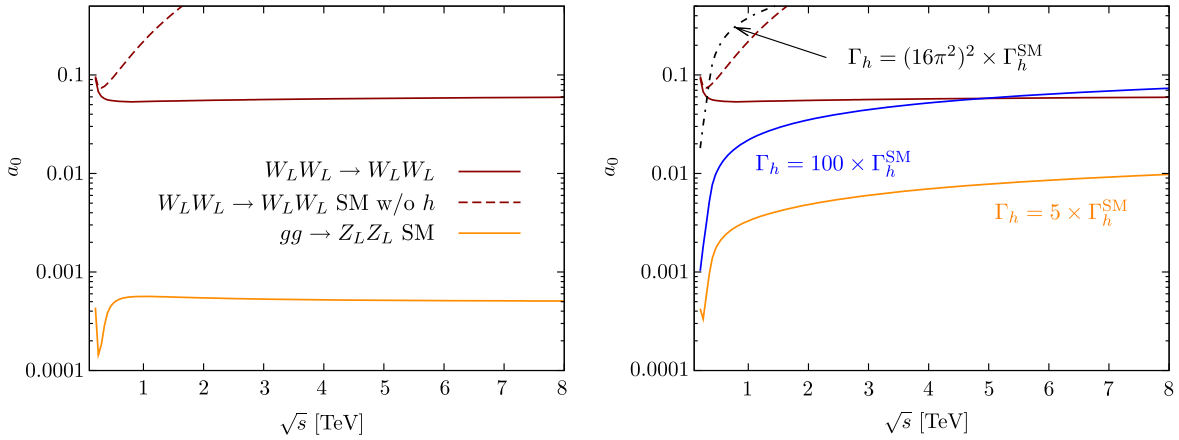

FIG. 5 (color online). Zeroth partial wave projection for $gg \to Z_LZ_L$ for the SM and various values of the $g_{ggh}g_{ZZh}$ rescaling as a consequence of $\mu = 1$ and $\Gamma_h > \Gamma_h^{\rm SM}$. We also show the partial wave projection for longitudinal WW scattering in the SM with and without Higgs to put $gg \to ZZ$ into context.

center-of-mass energy in Fig. 5. Unitarity is violated when $a_0 > 0.5$ [30], and to contextualize our $gg \to ZZ$ findings with the SM Higgs sector, we also show curves for SM W_LW_L scattering that violates unitarity at low scales if the Higgs contribution is neglected.

Indeed, the $gg \to Z_LZ_L$ scattering is sensitive to the coupling rescaling as can be seen from Fig. 5; however, the partial wave does not get close to 0.5. The amplitude is sufficiently diluted by loop factors $16\pi^2 \sim 160$. Once this factor is resolved, the unitarity bound becomes relevant. This, however, corresponds to a regime where the narrow width approximation is violated entirely.

Although the limit in this channels is not afflicted with probability nonconservation, it should be clear that the invoked rescaling leads to an ill-defined electroweak sector as demonstrated in Fig. 4; the triangle and box contributions remain intimately related. If high invariant mass measurements in the $gg \to ZZ$ channel yield a statistically significant increase over the SM, the interpretation in terms of a modified Higgs width becomes model dependent.

III. DECORRELATING ON-SHELL AND OFF-SHELL MEASUREMENTS IN BSM THEORIES

A. BSM contributions to Higgs production

The interplay in the absorptive parts of $gg \to ZZ$ linked by unitarity in the high invariant mass regime and nondecoupling of top loops tells us that the limit-setting procedure outlined in the Introduction is based on a consistency argument for the electroweak sector and is very specific to masses that are generated through chirality-changing interactions. This paves the way to construct a straightforward counterexample of the Higgs width measurement as outlined above.

Consider ϕ, a scalar **3** under $\mathrm{SU}(3)_C$, coupled to the Higgs sector via portal interactions (see, e.g., Ref. [31]):

$$\mathcal{L}_\phi = |D_\mu\phi|^2 - \tilde{m}_\phi^2|\phi|^2 - \lambda|\phi|^2|H|^2 + \cdots. \quad (5)$$

When the Higgs field obtains its vacuum expectation value v, the field ϕ induces a contribution to single-Higgs production due to the interaction $\lambda v|\phi|^2 h$, as shown in Fig. 6. The physical mass $m_\phi^2 = \tilde{m}_\phi^2 + \lambda v^2$ is essentially a free parameter $m_\phi^2 > 0$.

The new contribution gives an additional and potentially large constructive or destructive contribution to $gg \to h$, depending on the sign and size of λ [32]. To enforce SM-like signal strengths $\mu \simeq 1$, we need to introduce a compensating contribution to the Higgs width (this could be interpreted as a Higgs-portal dark matter realization), and we have $\Gamma_h > \Gamma_h^{\rm SM}$.

Due to the scalar and electroweak singlet nature of the new fields, we only change the triangle Higgs production contribution, while leaving the box $gg \to ZZ$ contributions unaltered. Note that for this particle there is no unitarity relation between the boxes and triangles. We show the individual contributions of the scalar color triplet in Fig. 3, which allows us to compare their behavior with the SM contributions. The scalar loops can easily be suppressed by 2 orders of magnitude, leaving absolute and interference contributions to the total hadronic cross section small for energetic events. This behavior is qualitatively known from supersymmetric scenarios [33] but has also been discussed in nonsupersymmetric models [31,32]; effectively, we have achieved a decorrelation of $g_{ggh}(m_h)$ and $g_{ggh}(m(ZZ) > m_h)$, and the measurement can no longer be interpreted as a Higgs width constraint.

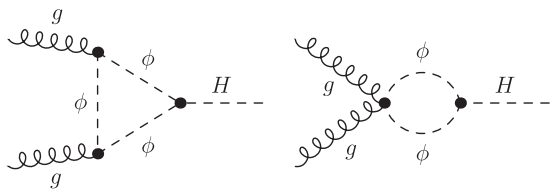

FIG. 6. New Feynman diagram topologies to Higgs production via gluon fusion arising from Eq. (5).

To qualitatively understand why the scalars are suppressed at large invariant masses, let us consider the ratio of the off-shell $gg \to h$ subamplitudes for scalars and tops (assuming $m_\phi = m_t = y_t v/\sqrt{2}$, $\lambda = y_t$ for simplicity):

$$y_t \frac{\mathcal{M}_\phi}{\mathcal{M}_t} = \frac{1 + 2m_t^2 C_0(s, m_t)}{(s - 4m_t^2) C_0(s, m_t) - 2}, \tag{6}$$

where $C_0(s, m_t^2)$ denotes the characteristic scalar three-point function following the Passarino-Veltman reduction [34]. The ϕ-induced amplitude is suppressed $\sim s^{-1}$, leading to a dominant behavior of the top loops at large momenta. This means that, even though we have a modified Higgs phenomenology at around $m_h \simeq 125$ GeV, it is exactly the decoupling of the Higgs width according to Eq. (3) which renders the high invariant mass measurement insensitive to modifications of Γ_h.

There is an interesting possibility when we consider larger ϕ masses and larger couplings λ. For invariant masses $s^2 \geq 4m_\phi^2$ we can have a sizeable constructive interference of the ϕ diagrams with the top loops, and as a result the cross section for large $m(4\ell)$ rises again, and we recover the qualitative behavior of Ref. [11]. For these parameter choices, however, we find that the excess is smaller than expected for rescalings of $g_{ggh} g_{ZZh}$ to keep $\mu \simeq 1$ (Table I). Similar effects show up for light spectra $m_\phi \lesssim 2m_t$, where this interference is destructive and the high invariant mass search region has a slightly smaller cross section, although $\Gamma_h/\Gamma_h^{\rm SM} \gg 1$ outside the current CMS exclusion.

In total, it is well possible to achieve $\Gamma_h \gg \Gamma_h^{\rm SM}$ without modifying the high invariant mass regime of $pp \to 4\ell$ and without running into unitarity issues as mentioned above. If such a contribution can be present, the Higgs width is an essentially unconstrained parameter, at least for a measurement as outlined in Refs. [11,18].

Even though Eq. (5) is a toy model to demonstrate the limitations of total Higgs width measurements in the $gg \to 4\ell$ channel, color triplets of this form appear in any supersymmetric BSM scenario, and our argument has a broad validity, see e.g. Refs. [33,36] for a discussion of squark contributions to Higgs production from gluon fusion in the MSSM. If the extra scalars are charged under flavor, e.g. they are top partners, exclusion will remain difficult [37] for the SUSY chimney regions (note that there are two chimney regions where one can hide 170 GeV and 70 GeV scalars). Despite being color charged, they could exist as stable particles on collider lifetimes when SUSY is relaxed [38]. Quite naturally, details quickly become highly model dependent. By fixing m_ϕ, we can map $\Gamma_h = 4.2 \times \Gamma_h^{\rm SM}$ onto λ and obtain $\bar{\sigma}/\bar{\sigma}^{\rm SM}$ in Table I. When the m_ϕ masses become heavy, we start approaching an effective theory limit, which quickly decouples unless we allow nonperturbative couplings, as m_ϕ is not generated via the Higgs mechanism. This is also visible in Fig. 3, and we recover the qualitative behavior of Ref. [11] also in this model as alluded to above. It is important to note, however, that the interpretation of the measurement is still far more complicated. If we imagine becoming sensitive to the SM tail distribution within a small error while observing a SM-like Higgs peak phenomenology, the mass constraints to decorrelate the on- and off-shell regions are weakened, and heavier colored bosons in this channel and scenario become essentially unconstrained.

Even though we have limited our discussion to $ZZ \to 4\ell$, the findings of this section straightforwardly generalize to $ZZ \to 2\ell 2\nu$ and WW.

TABLE I. Results for a single triplet scalar (5) giving the correlation between μ, $\Gamma_h/\Gamma_h^{\rm SM}$ and the high invariant mass cross section $\bar{\sigma}$ for the CMS selection cuts.

m_ϕ	μ (h peak)	$\Gamma_h/\Gamma_h^{\rm SM}$	$\bar{\sigma}/\bar{\sigma}^{\rm SM}$ $[m(4\ell) \geq 330$ GeV$]$[a]
70 GeV	$\simeq$1.0	$\simeq$5	−2%
170 GeV	$\simeq$1.0	$\simeq$4.7	+80%
170 GeV	$\simeq$1.0	$\simeq$1.7	+6%

[a]We impose the cut set used by CMS [18] without the MELA cut [35].

B. BSM contributions to continuum ZZ and WW production

Our previous example shows that new contributions to $gg \to h$ can significantly loosen the bounds on the Higgs width interpretation. In a similar fashion, we can imagine a situation where $\Gamma_h \neq \Gamma_h^{\rm SM}$ and the correlation of Eqs. (2) and (4) is changed by new contributions to continuum ZZ production. Such effects are expected in composite Higgs scenarios with vectorlike quarks [39] and typically have nontrivial and nondiagonal electroweak interactions in the extended flavor sector. In realistic models [40], such sectors can be quite large, and the phenomenology becomes nontransparent, especially when the different mass scales are resolved and effective field theory simplifications cannot be applied.

To keep our discussion as transparent as possible we will focus on a minimal, anomaly-free toy model of vectorlike quarks:

$$\begin{aligned} -\mathcal{L} \supset\ & m_Q \bar{Q}'_L Q''_R + m_d \bar{d}''_L d'_R + m_u \bar{u}''_L u'_R + \text{H.c.} \\ & + y'_d (\bar{Q}'_L H) d'_R + y'_u (\bar{Q}'_L i\sigma^2 H^\dagger) u'_R + \text{H.c.} \\ & + y''_d (\bar{Q}''_R H) d''_L + y''_u (\bar{Q}''_R i\sigma^2 H^\dagger) u''_L + \text{H.c.}, \end{aligned} \tag{7}$$

where Q'_L, $Q''_R = (\mathbf{3}, \mathbf{2}, -\frac{1}{2})$, d''_L, $d'_R = (\mathbf{3}, \mathbf{1}, -1)$, u''_L, $u'_R = (\mathbf{3}, \mathbf{1}, 0)$ under $\mathrm{SU}(3)_C \times \mathrm{SU}(2)_L \times \mathrm{U}(1)_Y$, i.e., we choose lepton hypercharge quantum numbers for simplicity. Depending on the relative size of the Yukawa coupling y_i, we can dial between the modifications in the triangle and box contributions, while the box contributions become sensitive to flavor-changing charged and neutral current interactions that follow from diagonalizing Eq. (7). In this sense, Eq. (7) reflects the qualitative features of more

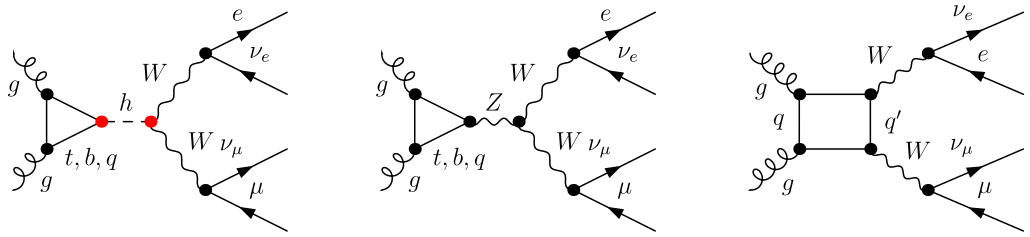

FIG. 7 (color online). Representative Feynman diagram topologies contributing to $gg \to WW$ with leptonic W-boson decays. QED contributions are identical to zero due to Furry's theorem [42]; the Z boson only probes an axial vector component.

realistic models and allows us to correlate the off-peak cross section with oblique parameter constraints.

Depending on the size of (non)diagonal couplings, we can, in principle, induce a new scale at large invariant ZZ or WW masses; see Figs. 2 and 7. In case the masses of these extra fermions are dominated by vectorial mass terms, oblique electroweak constraints [41] are largely insensitive to their presence. For $y_i \equiv 0$ we generically find $|S| \sim 10^{-3}$, $T = 0$ and $|U| \sim 10^{-2}$ over a broad range of parameter choices by explicit calculations. For pure vectorlike terms we find for the CMS search region described in Ref. [18] (neglecting again MELA cuts),

$$\Delta^{v}_{ZZ} \left.\frac{\bar{\sigma}^{\rm BSM} - \bar{\sigma}^{\rm SM}}{\bar{\sigma}^{\rm SM}}\right|_{ZZ} \simeq -4.8\%, \tag{8}$$

even for light physical fermion mass scales

$$(m_{d,1}, m_{d,2}, m_{u,1}, m_{u,2}) = (300, 200, 400, 300)\ \text{GeV}, \tag{9}$$

which are already under pressure from direct search exclusion limits. The fermions quickly decouple for larger masses, owing to the dimension-8 structure of the resulting effective theory. We can also define a high invariant $WW \to \ell\ell' 2\nu$ mass region that is characterized by a large value of the transverse mass

$$m_T^2 = (p_T + \not{p}_T)^2 - (\mathbf{p}_T + \not{\mathbf{p}}_T)^2, \tag{10}$$

and we choose $m_T \geq 300$ GeV in the following in addition to $p_T(\ell) \geq 10$ GeV, $|y_\ell| \leq 2.5$, $\Delta R(\ell\ell') \geq 0.2$ and $\not{p}_T \geq 20$ GeV. As can be seen in Fig. 7, WW has a qualitatively different sensitivity to this particular model class. We find in this region

$$\Delta^{v}_{WW} = \left.\frac{\bar{\sigma}^{\rm BSM} - \bar{\sigma}^{\rm SM}}{\bar{\sigma}^{\rm SM}}\right|_{WW} \simeq -3.8\%. \tag{11}$$

for our example mass point in Eq. (9).

To understand how far oblique correction constraints limit the size of novel electroweak degrees of freedom, we can use the above toy model and take the mass spectrum of Eq. (9) as a baseline. Then we change the "chiral" components by increasing $y_i \geq 0$ until we reach the boundary of the S, T exclusion ellipse [43]. For the resulting parameter point we obtain cross sections analogous to Eqs. (8) and (11):

$$\Delta^{v+h}_{ZZ} \simeq -4.3\%, \qquad \Delta^{v+h}_{WW} \simeq -3.7\%. \tag{12}$$

This example demonstrates that we can expect that large BSM contributions to the continuum ZZ production are highly limited by electroweak precision constraints, especially because they also link to nontrivial gauge representations under $\mathrm{SU}(3)_C$. The ZZ and WW production modes are directly correlated with S, T, U, and Higgs VEV-induced mass terms in Eq. (7) quickly introduce a tension with electroweak precision constraints. They are known to have a significant impact on $H \to \gamma\gamma$ [44] and can be resolved in precision experiments [45].

IV. HIGHER-DIMENSIONAL OPERATORS: IMPROVING $\mathcal{CP}$ SENSITIVITY

As a final application of the off-shell measurements, we discuss the impact of higher-dimensional operators [46,47] on such a measurement. A recent and comprehensive analysis has been presented in Ref. [19]. Here we limit ourselves to the investigation of $\mathcal{CP}$ properties, keeping all m_t, m_b dependencies, and show that differential information in the high invariant mass regime can be used to add a statistically independent measurement to the $\mathcal{CP}$ hypothesis test as already performed by ATLAS and CMS [48].

For this purpose, we focus on interactions

$$\mathcal{L} \supset \sum_{V=Z,W^+} c_{e,V} g_V m_V V^\dagger_\mu V^\mu h + \frac{c_{o,V}}{m_V^2} \tilde{V}^{\mu\nu} V_{\mu\nu} A \tag{13}$$

and define the physical Higgs boson as a linear combination of $\mathcal{CP}$-even and $\mathcal{CP}$-odd states,

$$X = \cos\alpha h + \sin\alpha A. \tag{14}$$

We fix the signal strength for different angles α by changing Γ_h accordingly and focus in the following on the two angles

$$\cos\theta_1 = \left.\frac{\mathbf{p}(e^+)\cdot\mathbf{p}_X}{\sqrt{\mathbf{p}^2(e^+)\mathbf{p}_X^2}}\right|_{Z\to e^+e^-}, \tag{15}$$

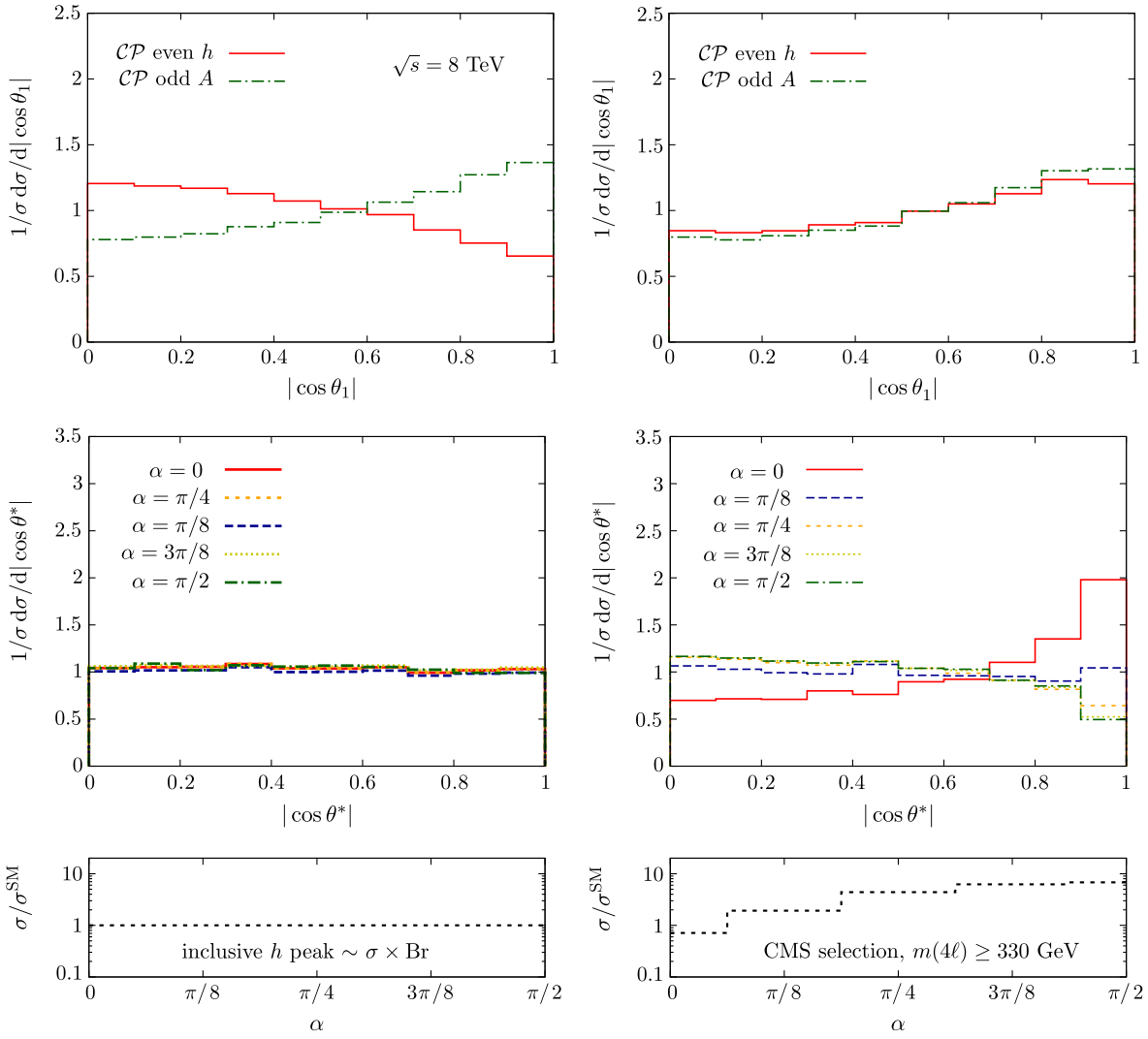

FIG. 8 (color online). $\cos\theta_1$ (top panels) and $\cos\theta^*$ distributions (middle panels) for the inclusive peak region and in the search region defined by CMS in Ref. [18]. α denotes the admixture of $\mathcal{CP}$-even vs $\mathcal{CP}$-odd; signal strengths $\mu \sim 1$ in the peak region are enforced via $\Gamma_h \neq \Gamma_h^{\rm SM}$. The lower panel shows the BSM to SM ratio for the different values of α.

$$\cos\theta^* = \left.\frac{\mathbf{p}(Z \to e^+e^-)\cdot\mathbf{b}}{\sqrt{\mathbf{p}^2(Z \to e^+e^-)\mathbf{b}^2}}\right|_X, \tag{16}$$

where $\ldots|_R$ refers to the rest frame R in which the angle is defined. $p_\mu(X) = p_\mu(e^+) + p_\mu(e^-) + p_\mu(\mu^+) + p_\mu(\mu^-)$ coincides in the on-shell region with the Higgs boson's rest frame, and $\mathbf{b}$ is an arbitrary three-vector along the positive beam direction. As defined, $\cos\theta^*$ correlates the production mechanism with the resonance's decay products by projecting onto the beam component of the four-lepton system. While $\cos\theta^*$ is known to be flat, $\cos\theta_1$ is sensitive to the $\mathcal{CP}$ properties of the Higgs boson when produced in the on-shell region, see Fig. 8 and Ref. [49]. As can be seen, on top of a cross-section increase due to the higher-dimensional operator structure [19], there is complementary information in the spin/$\mathcal{CP}$ observables.[5]

V. OFF-SHELL MEASUREMENTS IN WEAK BOSON FUSION

The potentially unknown loop contributions that can decorrelate the on-shell and off-shell regions in gluon fusion are not present in weak boson fusion, assuming indeed a $\mathcal{CP}$-even SM-like Higgs boson. In these channels, the method of Ref. [11] becomes largely model independent except for a potential asymmetric deviation of the WWh and ZZh

[5]Not included in Fig. 8 is the WBF contribution that can give rise to an additional ~10% effect. We have checked the angular distributions with a modified version of VBFNLO and find no significant impact on the quoted results.

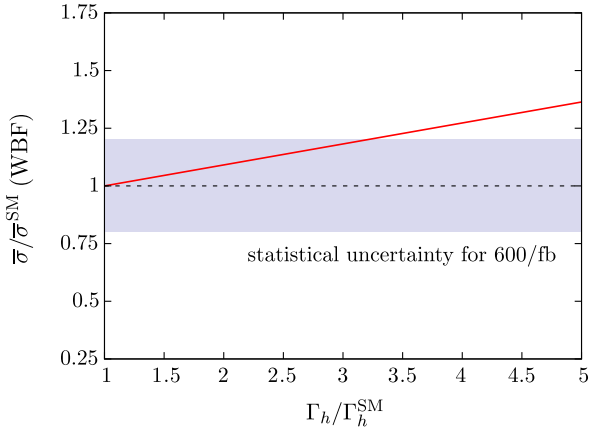

FIG. 9 (color online). Weak boson fusion analysis of the off-shell measurement of Ref. [11]. We apply hard weak boson fusion cuts to suppress a pollution from gluon fusion and include the statistical error based on a measurement with 600/fb. For details, see text.

couplings. This directly links to the T parameter, and a deviation at tree level is expected to be small.

Furthermore, the weak boson fusion topology allows us to suppress gluon fusion contributions using forward tagging jets in opposite detector hemispheres with large invariant mass and rapidity gap [50]. By imposing an additional central jet veto [51], the gluon fusion events are almost entirely removed from the sample [52], and the impact on a correlation of the on- and off-shell regions will be unaffected by unknown physics beyond the SM as a consequence.

In Fig. 9, we show the result of such an analysis at NLO QCD [24,53]. (We choose a common rescaling of g_{ZZh} and g_{WWh} to achieve $\mu \simeq 1$ in the on-peak region.) The selection cuts are identical to CMS's choice for the Z reconstruction and lepton selection. We lower the 4ℓ mass cut to $m(4\ell) \geq 130$ GeV to increase the statistics as much as possible. In addition, we employ typical WBF cuts [50,51,53] as outlined above,

$$p_T(j) > 20\ \text{GeV}, \quad \Delta R(jj) \geq 0.6, \quad |y_j| < 4.5, \quad \Delta y(jj) \geq 4.5, \quad y_{j_1} \times y_{j_2} < 0, \quad m(jj) \geq 800\ \text{GeV}, \tag{17}$$

and a jet veto

$$|y_j^{\rm veto}| < 2.5, \quad p_T^{\rm veto}(j) > 50\,\text{GeV}, \quad \Delta y(j_{\rm veto} j) > 0.3. \tag{18}$$

The leptons need to be well separated from the jets $\Delta R(\ell j) \geq 0.6$ and need to fall inside the tagging jets' rapidity gap. We furthermore reject events with $m(4\ell) > 2$ TeV to avoid picking up sensitivity from the region of phase space where the off-shell modification probes the unitarity-violating regime.

Obviously, when performed in the WBF channel (our reasoning also applies to the WW channel), we observe a similar behavior [12]; however, it is at a much smaller cross section $\bar{\sigma}(\text{WBF}) \simeq 0.04$ fb at 14 TeV (already summed over light lepton flavors $\ell = e, \mu$) [24]. Nonetheless, such a measurement can be used to obtain a fairly model-independent measurement of the total Higgs width following Ref. [11] at large integrated luminosity, especially when statistically independent information from multiple WBF channels is combined.

VI. SUMMARY AND CONCLUSIONS

After the Higgs discovery with a mass of $m_h \simeq 125$ GeV and TeV scale naturalness under siege, the total Higgs width is one of the most sensitive parameters to light physics beyond the standard model with a relation to the electroweak scale. A *model-independent* constraint on Γ_h would have a huge impact on BSM physics. Correlating on- and off-shell Higgs production in $gg \to ZZ$, WW and understanding cross section measurements in terms of a total Higgs width limit, however, only applies to the SM. Injecting the SM hypothesis into a global Higgs fit, however, will always yield much tighter constraints [4].

The on- and off-peak continuum regions can be decorrelated in gluon fusion by new degrees of freedom, which link to a modified Higgs phenomenology; large BSM effects in continuum $gg \to ZZ$, WW seem unlikely given existing electroweak precision constraints.

If deviations at large invariant masses for VV final states are observed in the future, unitarity of the scattering amplitude dictates that the interpretation of $\Gamma_h > \Gamma_h^{\rm SM}$ will need to involve model-specific assumptions, a fact that is unavoidable in hadron collider physics. The cross-section measurement can be used to constrain momentum-dependent modifications of Higgs couplings that underlie the modeling of spin/$\mathcal{CP}$ testing and the general limit setting procedure of higher-dimensional operators.

Applying the strategy of Ref. [11] to WBF allows us to formulate a constraint that is largely free of the gluon fusion shortcomings; however, at considerably smaller cross sections.

A precise model-independent constraint on the total Higgs width $\Gamma_h \simeq \Gamma_h^{\rm SM}$, if not a measurement of Γ_h, is challenging from a statistics and systematics point of view and probably remains the remit of a future theoretically and experimentally clean linear collider environment. At e.g. a 250 GeV e^+e^- machine, the combined investigation of associated and WBF Higgs production, and exclusive final states $H \to b\bar{b}$, WW allows us to formulate constraints on Γ_h in the 10% range [54].

ACKNOWLEDGMENTS

C. E. is supported by the Institute for Particle Physics Phenomenology Associateship program.

[1] G. Aad *et al.* (ATLAS Collaboration), Phys. Lett. B **716**, 1 (2012).

[2] S. Chatrchyan *et al.* (CMS Collaboration), Phys. Lett. B **716**, 30 (2012).

[3] A. Azatov, R. Contino, and J. Galloway, J. High Energy Phys. 04 (2012) 127; P. P. Giardino, K. Kannike, M. Raidal, and A. Strumia, Phys. Lett. B **718**, 469 (2012); J. Ellis and T. You, J. High Energy Phys. 09 (2012) 123; J. R. Espinosa, C. Grojean, M. Muhlleitner, and M. Trott, J. High Energy Phys. 12 (2012) 045; T. Plehn and M. Rauch, Europhys. Lett. **100**, 11002 (2012); T. Corbett, O. J. P. Eboli, J. Gonzalez-Fraile, and M. C. Gonzalez-Garcia, Phys. Rev. D **87**, 015022 (2013); E. Masso and V. Sanz, Phys. Rev. D **87**, 033001 (2013); A. Djouadi and G. Moreau, Eur. Phys. J. C **73**, 2512 (2013); P. Bechtle, S. Heinemeyer, O. Stal, T. Stefaniak, and G. Weiglein, arXiv:1403.1582.

[4] B. A. Dobrescu and J. D. Lykken, J. High Energy Phys. 02 (2013) 073; CMS Collaboration, Report No. CMS.PAS-HIG-13-005, 2013.

[5] A. Djouadi, A. Falkowski, Y. Mambrini, and J. Quevillon, Eur. Phys. J. C **73**, 2455 (2013).

[6] T. Binoth and J. J. van der Bij, Z. Phys. C **75**, 17 (1997); R. Schabinger and J. D. Wells, Phys. Rev. D **72**, 093007 (2005); B. Patt and F. Wilczek, arXiv:hep-ph/0605188.

[7] C. Englert, T. Plehn, M. Rauch, D. Zerwas, and P. M. Zerwas, Phys. Lett. B **707**, 512 (2012); G. M. Pruna and T. Robens, Phys. Rev. D **88**, 115012 (2013); S. Y. Choi, C. Englert, and P. M. Zerwas, Eur. Phys. J. C **73**, 2643 (2013); R. Foot, A. Kobakhidze, and R. R. Volkas, Phys. Rev. D **84**, 095032 (2011); R. Foot, Phys. Lett. B **728**, 45 (2014).

[8] C. Englert, E. Re, and M. Spannowsky, Phys. Rev. D **87**, 095014 (2013); K. Hartling, K. Kumar, and H. E. Logan, Phys. Rev. D **90**, 015007 (2014).

[9] C. Englert, E. Re, and M. Spannowsky, Phys. Rev. D **88**, 035024 (2013); Z. Kang, J. Li, T. Li, Y. Liu, and G.-Z. Ning, arXiv:1404.5207; C.-W. Chiang, A.-L. Kuo, and K. Yagyu, J. High Energy Phys. 10 (2013) 072; B. Grinstein, C. W. Murphy, D. Pirtskhalava, and P. Uttayarat, J. High Energy Phys. 05 (2014) 083.

[10] Atlas Collaboration, Report No. ATLAS-CONF-2013-011, 2013.

[11] F. Caola and K. Melnikov, Phys. Rev. D **88**, 054024 (2013).

[12] N. Kauer and G. Passarino, J. High Energy Phys. 08 (2012) 116; N. Kauer, J. High Energy Phys. 12 (2013) 082; Mod. Phys. Lett. A **28**, 1330015 (2013).

[13] J. M. Campbell, R. K. Ellis, and C. Williams, J. High Energy Phys. 04 (2014) 060.

[14] J. M. Campbell, R. K. Ellis, and C. Williams, Phys. Rev. D **89**, 053011 (2014).

[15] B. Coleppa, T. Mandal, and S. Mitra, arXiv:1401.4039.

[16] L. J. Dixon and Y. Li, Phys. Rev. Lett. **111**, 111802 (2013).

[17] L. J. Dixon and M. S. Siu, Phys. Rev. Lett. **90**, 252001 (2003); S. P. Martin, Phys. Rev. D **88**, 013004 (2013); **86**, 073016 (2012).

[18] CMS Collaboration, Report No. CMS-PAS-HIG-14-002, 2014.

[19] J. S. Gainer, J. Lykken, K. T. Matchev, S. Mrenna, and M. Park, arXiv:1403.4951.

[20] B. Grinstein, C. W. Murphy, and D. Pirtskhalava, J. High Energy Phys. 10 (2013) 077; Y. Chen, R. Harnik, and R. Vega-Morales, arXiv:1404.1336.

[21] T. Hahn and M. Perez-Victoria, Comput. Phys. Commun. **118**, 153 (1999); T. Hahn, Comput. Phys. Commun. **140**, 418 (2001); *Proc. Sci.*, ACAT (2010) 078.

[22] H. Murayama, I. Watanabe, and K. Hagiwara, Report No. KEK-91-11, 1992.

[23] J. Alwall, P. Demin, S. de Visscher, R. Frederix, M. Herquet, F. Maltoni, T. Plehn, D. L. Rainwater, and T. Stelzer, J. High Energy Phys. 09 (2007) 028; J. Alwall, M. Herquet, F. Maltoni, O. Mattelaer, and T. Stelzer, J. High Energy Phys. 06 (2011) 128.

[24] K. Arnold, M. Bahr, G. Bozzi, F. Campanario, C. Englert, T. Figy, N. Greiner, C. Hackstein *et al.*, Comput. Phys. Commun. **180**, 1661 (2009).

[25] J. R. Ellis, M. K. Gaillard, and D. V. Nanopoulos, Nucl. Phys. **B106**, 292 (1976); M. A. Shifman, A. I. Vainshtein, M. B. Voloshin, and V. I. Zakharov, Yad. Fiz. **30**, 1368 (1979) [Sov. J. Nucl. Phys. **30**, 711 (1979)]; B. A. Kniehl and M. Spira, Z. Phys. C **69**, 77 (1995).

[26] R. E. Cutkosky, J. Math. Phys. (N.Y.) **1**, 429 (1960).

[27] M. S. Chanowitz, M. A. Furman, and I. Hinchliffe, Phys. Lett. B **78**, 285 (1978); Nucl. Phys. **B153**, 402 (1979).

[28] S. Heinemeyer *et al.* (LHC Higgs Cross Section Working Group), arXiv:1307.1347.

[29] M. Ciccolini, A. Denner, and S. Dittmaier, Phys. Rev. Lett. **99**, 161803 (2007); M. Ciccolini, A. Denner, and S. Dittmaier, Phys. Rev. D **77**, 013002 (2008).

[30] M. Jacob and G. C. Wick, Ann. Phys. (N.Y.) **7**, 404 (1959); **281**, 774 (2000).

[31] K. Kumar, R. Vega-Morales, and F. Yu, Phys. Rev. D **86**, 113002 (2012).

[32] B. A. Dobrescu, G. D. Kribs, and A. Martin, Phys. Rev. D **85**, 074031 (2012).

[33] R. Bonciani, G. Degrassi, and A. Vicini, J. High Energy Phys. 11 (2007) 095.

[34] G. 't Hooft and M. J. G. Veltman, Nucl. Phys. **B153**, 365 (1979); G. Passarino and M. J. G. Veltman, Nucl. Phys. **B160**, 151 (1979); A. Denner, Fortschr. Phys. **41**, 307 (1993).

[35] S. Chatrchyan *et al.* (CMS Collaboration), Phys. Lett. B **716**, 30 (2012).

[36] C. Anastasiou, S. Beerli, S. Bucherer, A. Daleo, and Z. Kunszt, J. High Energy Phys. 01 (2007) 082; U. Aglietti, R. Bonciani, G. Degrassi, and A. Vicini, J. High Energy Phys. 01 (2007) 021; M. Mühlleitner and M. Spira, Nucl. Phys. **B790**, 1 (2008).

[37] See e.g. the combination of CMS Collaboration, Reports No. SUS-13-004, No. SUS-13-011, and No. SUS-13-011.

[38] B. Batell, J. Pradler, and M. Spannowsky, J. High Energy Phys. 08 (2011) 038.

[39] P. Lodone, J. High Energy Phys. 12 (2008) 029.

[40] R. Contino, L. Da Rold, and A. Pomarol, Phys. Rev. D **75**, 055014 (2007); M. Gillioz, R. Grober, C. Grojean, M. Muhlleitner, and E. Salvioni, J. High Energy Phys. 10 (2012) 004; M. Gillioz, R. Grober, A. Kapuvari, and M. Muhlleitner, J. High Energy Phys. 03 (2014) 037.

[41] M. E. Peskin and T. Takeuchi, Phys. Rev. D **46**, 381 (1992); Phys. Rev. Lett. **65**, 964 (1990).

[42] W. H. Furry, Phys. Rev. **51**, 125 (1937).
[43] H. Flacher, M. Goebel, J. Haller, A. Hocker, K. Monig, and J. Stelzer, Eur. Phys. J. C **60**, 543 (2009); **71**, 1718(E) (2011).
[44] A. Joglekar, P. Schwaller, and C. E. M. Wagner, J. High Energy Phys. 12 (2012) 064.
[45] C. Englert and M. McCullough, J. High Energy Phys. 07 (2013) 168.
[46] K. Hagiwara, R. D. Peccei, D. Zeppenfeld, and K. Hikasa, Nucl. Phys. **B282**, 253 (1987); V. Barger, T. Han, P. Langacker, B. McElrath, and P. Zerwas, Phys. Rev. D **67**, 115001 (2003).
[47] A. Alloul, B. Fuks, and V. Sanz, J. High Energy Phys. 04 (2014) 110.
[48] CMS Collaboration, Phys. Rev. Lett. **110**, 081803 (2013); ATLAS Collaboration, Phys. Lett. B **726**, 120 (2013).
[49] For recent work, see S. Y. Choi, D. J. Miller, M. M. Muhlleitner, and P. M. Zerwas, Phys. Lett. B **553**, 61 (2003); A. V. Gritsan, Z. Guo, K. Melnikov, M. Schulze, and N. V. Tran, Phys. Rev. D **81**, 075022 (2010); C. Englert, C. Hackstein, and M. Spannowsky, Phys. Rev. D **82**, 114024 (2010).
[50] D. L. Rainwater and D. Zeppenfeld, Phys. Rev. D **60**, 113004 (1999); **61**, 099901(E) (2000).
[51] V. D. Barger, R. J. N. Phillips, and D. Zeppenfeld, Phys. Lett. B **346**, 106 (1995).
[52] V. Del Duca, W. Kilgore, C. Oleari, C. Schmidt, and D. Zeppenfeld, Phys. Rev. Lett. **87**, 122001 (2001).
[53] B. Jager, C. Oleari, and D. Zeppenfeld, Phys. Rev. D **73**, 113006 (2006).
[54] C. Dürig, K. Fujii, J. List, and J. Tian, arXiv:1403.7734; H. Baer, T. Barklow, K. Fujii, Y. Gao, A. Hoang, S. Kanemura, J. List, H. E. Logan *et al.*, arXiv:1306.6352.